Chapter 1

SENSITIVITY OF STRUCTURAL RESPONSE TO WIND TURBULENCE CHARACTERISTICS

Vincent Denoël[*]
University of Liège, Belgium

August 3, 2010

PACS - 47.27.E- Turbulence simulation and modeling - 47.85.Gj Aerodynamics - 02.50.Cw Probability theory

Keywords: non Gaussian, bispectrum, correlation, wind loading, nonlinear, wind incidence, bridge deck.

AMS Subject Classification: -.

Abstract

Civil engineering structures that are built in the atmospheric boundary layer have to be designed according to the gusty winds they are likely to withstand during their lifetime. Traditionally statistical characteristics of the wind turbulence -as standard deviation of and correlation between turbulence components, frequency content, etc.

[*] ***E-mail address: v.denoel@ulg.ac.be***

- are provided to structural engineers by meteorologists. The first dialogue between these two communities dates back to 1960's when they agreed on a list of necessary statistical characteristics of turbulence that need to be observed and measured to feed the structural models available at that time. In the framework of advanced wind loading models developed recently, it turns out that this basic list of statistical characteristics of turbulence is no longer sufficient.
In this chapter, we point out some quantities that would need to be measured and others that are already measured but require a more precise estimation. This need is justified by analyzing the sensitivity, to these quantities, of the structural response to an advanced wind loading model.
After having introduced the need for advanced modeling of the wind loading, and eventually thus of the wind turbulence, a nonlinear non-Gaussian quasi-steady loading model is presented. Then the model is rigorously analyzed with cumbersome mathematics and statistics, with the permanent background aim at estimation of the influence of the turbulence properties. Final results are however presented in a concise way in order to pave the way for the future dialogue between engineers and meteorologists, and so build up the advanced design procedures that will presumably be used during the coming decades.

1. Introduction

A body immersed in a fluid flow is subjected to pressures resulting from the deviation of the flow around it. So is the case of civil engineering structures. Moreover, when the considered body is flexible, i.e. susceptible of moving in the fluid flow under the action of these pressures, its motion generates moving boundary conditions which perturb the flow. Pressures applied on the body are consequently modified and this ultimately results in a fluid-structure interaction. From a modeling viewpoint, this coupling requires solving simultaneously the fluid equations (Navier-Stokes) and the continuum equations (Theory of Elasticity).

In this picture, turbulence takes place at two levels. First, under consideration of structures in the atmospheric boundary layer, the wind flow is a high-Reynolds fluid flow and the turbulent upstream wind creates therefore time-dependent forces on the considered body. Second the bluffness of the considered body, a typical feature of civil structures, exacerbates the triggering of a turbulent wake. It is commonly accepted that the motion of the body in the fluid flow strongly influences these signature effects. An accurate determination of the time-space pattern of the wake needs therefore to be studied by means of adequate fluid-structure interaction simulations.

The design of civil engineering structures needs to embody these two aspects of turbulence [1, 2, 3]. Nevertheless, designers are essentially interested in pressures acting on structures and the features of the outward fluid flow are usually of relative importance, if not left behind to fluid dynamists. In caricatural structural engineers' opinion, fluid-structure analyses typically provide an exhaustive and confusing information, sometimes with a questionable pertinence. Moreover, the coupled analysis of a long bridge or high building would still require weeks of computation, even on supercomputers. Today, fluid-structure interaction models are rather devoted to the simulation of typical bridge/building cross sections, i.e. the study of only a limited part of the structure, similarly to what is done in the aeronautic industry where typical wing cross sections are modeled rather than whole airplanes.

Consequently, it turns out that experimental characterization by means of wind-tunnel tests remains a reference when wake effects and other aeroelastic phenomena have to be studied precisely.

On the contrary, the structural analysis under the second kind of turbulence, i.e. a turbulent oncoming flow, so-called buffeting analysis, has been modeled and studied for more than fifty years. In this context, the solution of Navier-Stokes equations is avoided and the turbulence is considered as an external loading, obviously random and henceforth characterized by means of probabilistic quantities. Within this framework, the assumptions of *linear* structural behavior as well as *stationarity* and *Gaussianity* of the turbulent loading have been accepted since the very early developments of these theories [4]. Actually this combination of assumptions is a key issue that allowed stochastic dynamic analyses to be performed fifty years ago. Indeed, the advantages of a frequency approach in a modal basis gave the opportunity to analyze large finite element structures. Although the original single mode method was improved to multiple modes [5, 6, 7], with uncorrelated then correlated modal responses, the three assumptions have so to speak never been reappraised. This pseudo-sedentary context enabled meteorologist and structural engineers to agree on the complete statistical description of the atmospheric turbulence that is necessary to feed this simple analysis model [8]. It consists in a Gaussian random field with correlation in time and coherence in space. This description is presented in more detail in Section 3.1..

It should be added that assumptions of linearity, stationarity and Gaussianity were specifically formulated in days where the computational possibilities were tremendously lower than what is available today. With a retrospective overlook , we may consider that the last fifty years were just the start-up period of buffeting analysis and that the twenty-first century will offer the computational means to tackle more realistic problems involving one or several of the so far assumed limitations. Some noticeable contributions have already been proposed in order to accommodate the buffeting model with a nonlinear structural behavior [9, 10, 11, 12], or non-stationary wind pressures [13, 14, 15, 16]. In this chapter we envisage the nonlinearity of aerodynamic forces, which results in a non Gaussian wind loading. The considered turbulence model is the Gaussian field for want of anything better, but it is evident that a more accurate representation of the turbulence (by means of a non Gaussian random field as it is most likely the case) would allow to better focus on the special features of the statistical properties of turbulence. In other words, because of the nonlinearity of the aerodynamic forces, a more accurate non Gaussian turbulence field could be considered at no extra cost, compared to the advanced non Gaussian structural analysis available today. Aiming at an expansion of the domain of applicability of this non Gaussian structural analysis model, we address in this chapter the problem of highlighting the required non Gaussian statistical properties of the atmospheric turbulence.

The most direct route to the characterization of wind forces is evidently to post-process pressure data, whenever they are available (wind tunnel or CFD results). Next we consider a variant of this characterization, because emphasis here is put on turbulence modeling, where the random forces are expressed via random pressures, which are themselves expressed as a quasi-steady transformation of the random velocity field of turbulence.

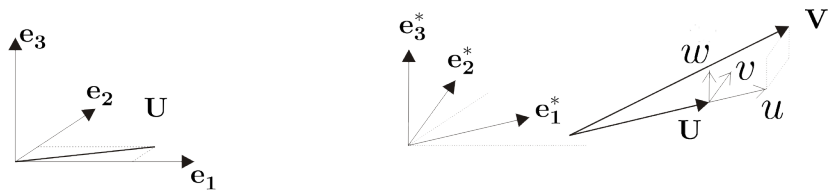

(a) (b)

Figure 1. Cartesian reference system $(\mathbf{e_1}, \mathbf{e_2}, \mathbf{e_3})$ and another fixed reference system $(\mathbf{e_1^*}, \mathbf{e_2^*}, \mathbf{e_3^*})$ oriented with respect to the mean wind direction.

2. Probabilistic Turbulence Model

Let $(\mathbf{e_1}, \mathbf{e_2}, \mathbf{e_3})$ a Cartesian reference system, with $\mathbf{e_3}$ pointing upward, see Fig. 1. The wind velocity $\mathbf{V}(\mathbf{x}, t)$ at a given point $\mathbf{x} \equiv (x_1, x_2, x_3)$ in space is supposed to be a stationary random field. Without any loss of generality, it may therefore be written as the sum of a mean velocity $\mathbf{U}(\mathbf{x})$ (computed on a period of time much longer than the time-scale of the turbulence, so typically 10 minutes) and fluctuations $\mathbf{u}(\mathbf{x}, t)$ around the mean velocity

$$\mathbf{V} = \mathbf{U} + \mathbf{u}. \tag{1}$$

In flat terrain where the mean wind flow is horizontal, a local reference system is defined with respect to the mean flow as

$$\mathbf{e_1^*} = \frac{\mathbf{U}}{|\mathbf{U}|}; \quad \mathbf{e_2^*} = \mathbf{e_3} \times \mathbf{e_1^*}; \quad \mathbf{e_3^*} = \mathbf{e_3} \tag{2}$$

in such a way that

$$\mathbf{U} = (U, \quad 0, \quad 0)^T \quad ; \quad \mathbf{u} = (u, v, w)^T \tag{3}$$

in $(\mathbf{e_1^*}, \mathbf{e_2^*}, \mathbf{e_3^*})$. The introduction of this new reference system allows interpreting u, v and w as the (zero mean) longitudinal, transverse horizontal and vertical components of the turbulence. Because the mean wind direction may change from place to place in space, we however need to concede that this referential may vary in space. In typical applications however, the space is divided into three to five zones at most, and the referential system is supposed to be constant throughout each zone.

Locally the turbulence is therefore represented by three random processes u, v and w. Their formal probabilistic description requires to characterize unilateral quantities as well as crossed probabilistic quantities between different components, and different spots in space. They are detailed in this Section.

2.1. Unilateral probabilistic description of turbulence

The exhaustive description of a random process u is given by its *multi-rank probability density function* $p_u^{(\infty)} = p_u(u_1, t_1; u_2, t_2; ...)$ which represents a scaled probability that the process u concurrently takes values in $[u_k, u_k + du_k]$ at times t_k, for $k = 1, ..., \infty$. For experimental reasons, it is difficult to identify this joint probability density function (pdf) for ranks larger than four or five [17]. The description of the components of the turbulence

are however usually limited to the second rank pdf [18, 1]. In this framework, the time delay $\Delta t = t_2 - t_1$ is introduced, and on account of the assumed stationarity of the turbulence, the second rank pdf writes

$$p_u^{(2)} = p_u\left(u_1; u_2, \Delta t\right) \tag{4}$$

with the meaning of a joint probability density function of the considered component of turbulence at two times delayed by Δt. In order to condensate the information in this function, it is usually replaced by some mathematical expectation

$$E\left[g\left(u_1, u_2\right)\right] = \int_{-\infty}^{+\infty}\int_{-\infty}^{+\infty} g\left(u_1, u_2\right) p_u^{(2)}(u_1; u_2, \Delta t) du_1\, du_2. \tag{5}$$

Central moments are the expectations obtained for $g = u_1^i u_2^j$ (u is a zero-mean process). Among them, the autocorrelation, obtained for $i = j = 1$, i.e. $R_u\left(\Delta t\right) = E\left[u_1 u_2\right]$, play a pivotal role. We may notice at this stage that the first rank pdf is recovered by considering all possible values for u_2, i.e. by integrating along u_2

$$p_u^{(1)} = \int_{-\infty}^{+\infty} p_u^{(2)}\left(u_1; u_2, \Delta t\right)\, du_2. \tag{6}$$

In wind engineering applications, for simplicity, $p_u^{(1)}\left(u_1\right)$ is usually considered to be the (zero mean) Gaussian distribution and is therefore explicitly determined by its standard deviation σ_u. Furthermore, the joint pdf $p_u^{(2)}\left(u_1\right)$ is assumed to be the bivariate Gaussian distribution with identical marginal distributions for u_1 and u_2, because of stationarity, and a correlation coefficient $\rho_u\left(\Delta t\right)$, i.e.

$$p_u^{(2)}\left(u_1, u_2, \Delta t\right) = \frac{1}{2\pi\sigma_u^2\sqrt{1-\rho_u^2\left(\Delta t\right)}} \mathrm{e}^{-\frac{u_1^2 - 2\rho_u(\Delta t)u_1 u_2 + u_2^2}{2\sigma_u^2\left(1-\rho_u^2(\Delta t)\right)}}. \tag{7}$$

It is straightforward to prove [19] that the correlation coefficient is related to the autocovariance through

$$\rho_u\left(\Delta t\right) = \frac{R_u\left(\Delta t\right)}{\sigma_u^2}. \tag{8}$$

Because $\rho_u(0) = 1$, the autocovariance function encapsulates information about σ_u^2 (the intercept of the autocovariance function). An alternative representation of the autocorrelation function is the power spectral density (psd), defined as its Fourier transform

$$S_u(\omega) = \frac{1}{2\pi}\int_{-\infty}^{+\infty} R_u(\tau) e^{-i\omega\tau} d\tau. \tag{9}$$

This representation is preferred by structural engineers because the structural analysis is usually conducted in the frequency domain. There are also evidences that the turbulence may advantageously be considered as a set of eddies with a continuum of wavelength, see for instance the famous Kolmogorov cascade [20].

Under so-called ergodic conditions, the psd of a turbulence component may be expressed as a function of the Fourier transform $\mathcal{F}_T\left[u\right]$ of an ideal realization of the random process

$$S_u\left(\omega\right) = \lim_{T\to\infty} \frac{2\pi}{T} \left\|\mathcal{F}_T\left[u\right]\right\|^2 \tag{10}$$

where T represents the duration of the considered realization. Ergodic conditions are always supposed to be met; the psd of turbulence components are basically estimated from experimental measurements with (10) where the measured signals are long enough so that the limit for $T \to \infty$ is supposed to be reached. Many theoretical models of the turbulence psd are available. The interested reader may refer to [3, 8] for commonly adopted expressions.

In summary, in the context of Gaussian turbulence, only one quantity, the psd, is provided for each turbulence component in order to fully characterize them. In particular, from definition (9) and its inverse Fourier transform, it is possible to prove that the integral of S_u along frequencies corresponds to the variance of the process

$$\sigma_u^2 = \int_{-\infty}^{+\infty} S_u(\omega)\, d\omega. \tag{11}$$

This illustrates again that a second rank quantity (psd) embeds first rank ones (variance).

2.2. Crossed probabilistic description of turbulence

Because they follow from the same phenomenology, the three components of the turbulence at the same location in space are not totally independent. Their first rank mutual interdependence is quantified by means of a correlation coefficient. Three coefficients are distinguished ρ_{uv}, ρ_{uw}, ρ_{vw} but only the second one is typically assumed to be non zero [21, 8]. Again, these first rank scalar quantities are associated to second rank functions, namely the cross-correlations $R_{uv}(\Delta t)$, $R_{uw}(\Delta t)$ and $R_{vw}(\Delta t)$ and the cross power spectral densities $S_{uv}(\omega)$, $S_{uw}(\omega)$ and $S_{vw}(\omega)$. For reasons similar to those mentioned above, the latter ones are essentially considered in practice and correlation coefficients are recovered by integration along frequencies. In the framework of Gaussian turbulence, the cross-psd's are the necessary and sufficient information to fully describe the joint statistics of the different components of turbulence; and again, various models are available.

The crossed probabilistic description of turbulence addresses also the correlation/coherence of turbulence components at various locations in space. In the frequency domain, it is represented by a coherence function $\Gamma(\omega)$, about which everyone agrees that it globally needs to decrease with frequency, as, for a given distance between two measurement points, high frequencies are attributable to small eddies that are less likely to bring coherence between both measurements. It seems however that there is no universal agreement on the particular expression of coherence functions: real or complex, exponentially decaying/based on Bessel functions, experimental/theoretical/semi-empirical [8]. In the framework of a Gaussian turbulence, the cross-psd's of the turbulence components between various points in the space are strictly sufficient to provide an exact description of the stochastic processes.

For the sake of conciseness in the notations, the unilateral and cross-psd's are gathered in a psd-matrix, as

$$\mathbf{S_u}(\omega) = \begin{bmatrix} S_u(\omega) & S_{vu}(\omega) & S_{wu}(\omega) \\ S_{uv}(\omega) & S_v(\omega) & S_{wv}(\omega) \\ S_{uw}(\omega) & S_{vw}(\omega) & S_w(\omega) \end{bmatrix}. \tag{12}$$

More generally, any random field, as (u, v, w) here, is characterized by a psd-matrix.

2.3. Higher rank description of the turbulence

Several wind-tunnel tests, field measurements and numerical simulations [22, 23, 24, 25] have revealed the non Gaussian nature of turbulence. Apparently, consideration of Gaussian wind velocity and acceleration is not a realistic statement. For instance, estimates of the probability density function $p_u^{(1)}$ obtained from real wind data indicate a significant skewness, i.e. non-zero third order probabilistic moment. However, the first rank pdf $p_u^{(1)}(u_1)$ does not contain an exhaustive information about the frequency distribution of the third probabilistic moment. Nor does the second rank pdf $p_u^{(2)}(u_1)$. In fact a rank-m pdf does not contain the frequency distribution of a statistical moment of order n, with $n > m$. With this respect, exactly as the second rank properties (psd/autocorrelation) have to be considered in order to characterize the frequency distribution of the variance (second moment), third rank properties, the bispectrum and the bicorrelation, need to be considered for the frequency distribution of the third moment [19].

As a matter of fact, this distribution is of paramount importance because the structural analysis under consideration here is a dynamic analysis where the structure is susceptible of exhibiting resonance phenomena. So, let us come back to the multi-rank probability density function $p_u^{(\infty)}$ and (marginally) integrate it now to the third rank pdf $p_u^{(3)}$. Because of stationarity, the three arguments t_1, t_2, t_3 may be replaced by two delays $\Delta t_1 = t_2 - t_1$ and $\Delta t_2 = t_3 - t_1$ such that

$$p_u^{(3)} = p_u\left(u_1; u_2, \Delta t_1; u_3, \Delta t_2\right). \tag{13}$$

This function definitely encloses much information, as for instance the second and first rank pdf (by integration along u_3), and a series of moments as

$$E\left[f\left(u_1, u_2, u_3\right)\right] = \iiint_{-\infty}^{+\infty} f\left(u_1, u_2, u_3\right) p_u^{(3)}\left(u_1; u_2, \Delta t_1; u_3, \Delta t_2\right) du_1\, du_2\, du_3. \tag{14}$$

Selection of $f = u_1^j u_2^j u_3^k$ with $k = 0$ shows that second rank moments as the autocorrelation function are enfolded in the third rank pdf. Of more importance is the bicorrelation, obtained for $i = j = k = 1$ and thus defined as

$$B_u\left(\Delta t_1, \Delta t_2\right) = E\left[u_1 u_2 u_3\right]. \tag{15}$$

The value of $B_u(0,0)$ at the origin corresponds to the third central moment μ_3, exactly as $R_u(0) = \mu_2 = \sigma_u^2$. For practical purposes, the two-fold Fourier transform of the bicorrelation, namely the bispectrum $D_u(\omega_1, \omega_2)$, is used as an alternative representation of the third rank properties

$$D_u\left(\omega_1, \omega_2\right) = \frac{1}{4\pi^2} \iint_{-\infty}^{+\infty} B_u\left(\tau_1, \tau_2\right) e^{-i\omega_1\tau_1} e^{-i\omega_2\tau_2} d\tau_1 d\tau_2 \tag{16}$$

and, similarly to (11), the third central moment is obtained as

$$\mu_3 = \iint_{-\infty}^{+\infty} D_u\left(\omega_1, \omega_2\right) d\omega_1 d\omega_2. \tag{17}$$

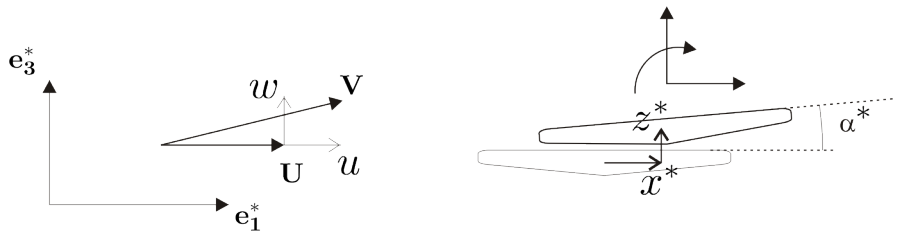

Figure 2. Components u and w of the 2-D wind turbulence and forces generated on a body immersed in the turbulent fluid flow.

This is the first function that represents the frequency distribution of the non Gaussian turbulence. Similar functions exist for higher orders (trispectrum, etc.). Despite the evidence that the wind turbulence is not a Gaussian process, very few information is available in the literature concerning realistic expressions of D_u.

2.4. Short summary

This short glossary of the statistical terms that will be used in the following sections was introduced in the context of atmospheric turbulence. Actually, any other kind of random field or random process is characterized by means of similar quantities. One could thus simply change the indices used in the previous two sections and consider therefore that other random processes are rather being surveyed. For instance, a random structural analysis consists in determining the statistical characteristics (of any rank) of the structural response. They are naturally described by means of their unilateral and cross-psd's, all gathered together in $\mathbf{S}_x$ (the psd matrix of the structural response), as well as higher rank properties in the context of a non-Gaussian description of the response.

3. Non Gaussian Forces Induced by Turbulence

3.1. Origins of Non Gaussianity

Pressures applied by the fluid flow around a body immersed therein are commonly integrated along the external surface of the body to yield six components, three forces and three moments of the aerodynamic tensor. They may be expressed at the center of gravity of the body, or more usually at the aerodynamic center (the point at which the pitching moment coefficient does not vary with the angle of attack, approximately the quarter-chord point for symmetric profiles).

In a quasi-steady context, each of these components is expressed as [2]

$$F = \frac{1}{2}\rho C\, B\, \|\mathbf{v}\|^2 \tag{18}$$

where ρ is the air density, B is a characteristic surface or volume and $\mathbf{v}$ is the relative velocity of the wind respect to the structure, which is expressed in the reference system

$(\mathbf{e_1^*}, \mathbf{e_2^*}, \mathbf{e_3^*})$ as

$$\mathbf{v} = \begin{pmatrix} U + u - x^* \\ v - y^* \\ w - z^* \end{pmatrix} \tag{19}$$

where x^*, y^* and z^* are the components of the body velocity in the local wind frame. For the sake of simplicity, we will consider next that the wind flow is 2-D, in the $(\mathbf{e_1^*}, \mathbf{e_3^*})$ plane. The wind incidence is therefore expressed as, see Fig. 2,

$$i = \arctan \frac{w - z^*}{U + u - x^*} - \alpha^*. \tag{20}$$

The aerodynamic coefficient C introduced in (18) corresponds to a particular component of the aerodynamic loading. For complex body shapes, it is usually measured in wind-tunnels although recent advances in CFD offer now rather good estimates. The aerodynamic coefficient is typically dependent of the shape of the considered body, but also, for a given body, to its orientation with respect to the oncoming flow. In other words, the aerodynamic coefficient measured on a fixed given body depends on the wind incidence. A simple expression is [26]

$$C(i) = \sum_{k=0}^{p} c_k i^k. \tag{21}$$

The quasi-steady nonlinear loading model is obtained by substitution of (19)-(21) into (18). From a first rank point of view, we may already concede that this nonlinear transformation of the random processes related to turbulence components u, v and w results in a non Gaussian aerodynamic loading, regardless of the consideration of u, v and w as possible non Gaussian processes.

From the above equations of the quasi-steady aerodynamic loading, we observe indeed that the origin of non Gaussianity is essentially two-fold: (i) from the intrinsic properties of the turbulence, and (ii) from the nonlinear factors in (18), namely the squared relative velocity, the nonlinear geometric expression of the angle of attack and the nonlinear aerodynamic coefficient. The first feature is not included in structural analyses today, mainly because of the lack of knowledge about bispectrum and trispectrum of turbulence. Concerning the second feature, several advanced models exist that encapsulate one or several of the three nonlinear expressions. These models are qualified as *advanced* because the majority of the analyses performed today still hinges on a Gaussian turbulence and linearized expressions of the three nonlinear factors.

In Section 3.3., we will show how a structural dynamical analysis may be conducted under non Gaussian loading. There is no doubt that the analysis method is applicable no matter the origin of the non Gaussianity, i.e. intrinsic to turbulence or not. The analysis tools are therefore ready to accommodate for a more precise description of the turbulence and we may therefore claim that a more sophisticated turbulence model could be granted in the design procedure at no significant extra cost.

3.2. Extremes of Non Gaussian processes

The non Gaussian nature of a random process is usually assessed by its cumulants of orders higher than two. The influence of the third cumulant/moment is to skew the probability

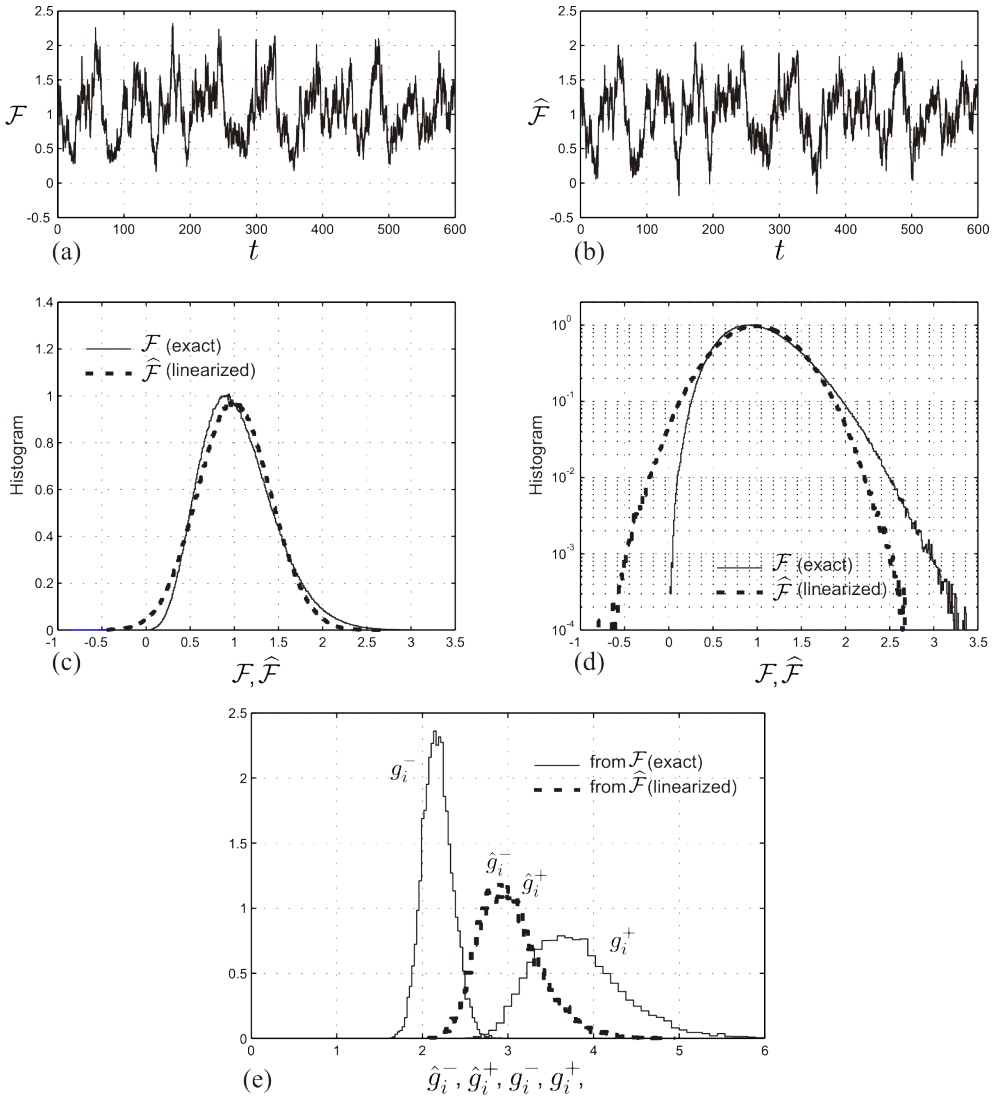

Figure 3. Extreme values of Gaussian and non-Gaussian processes. This figure shows that the linearized aerodynamic force underestimates extreme forces (square Gaussian process with small intensity): realizations of a non-Gaussian (a) and Gaussian (b) aerodynamic force signal; histograms of the force in Cartesian (c) and logarithmic (d) plots; probability distribution of the extreme values (e), in terms of peak factors.

distribution to the left or to the right, and consequently to affect the distribution in the tails of the pdf. This results in a more or less significant modification of extreme values, i.e. those that are precisely considered for a design. This simple deduction on a first-rank quantity (the pdf) actually needs to be complemented in order to formally establish the statistics of extreme values. Extreme values are defined as the expected maximum (or minimum) of a random process, given an observation window length T. Sophisticated analytical models have been developed in the context of Gaussian processes and more recently extended to some classes of non Gaussian processes. The purpose of this section is not to present or compare available methods, but well to illustrate the influence of the non Gaussian nature of random processes on their extreme values.

For this purpose, a 1-D turbulent flow is considered ($v = w = 0$) and its frequency content is obtained as a first order autoregressive filtering of a delta correlated noise e as

$$u_{i+1} = a\, u_i + (1-a)\, e_i \quad \text{with } i = 1, ...N. \tag{22}$$

The filtering parameter a is obtained as $a = 1+\beta/2-\sqrt{\beta\,(1+\beta/4)}$ with $\beta = \alpha^2\Delta t^2$, where α is a characteristic frequency and Δt is the time step used for the generation. A realistic choice for atmospheric turbulence is $\alpha = 0.1$ rad/s, see [27], and we sample it here with $\Delta t = 0.1s$. The number of points in the synthetic realization of the wind flow is $N = 6,000$, so as to generate a 10 minute long sample, in accordance with common practice. Notice that the generation is performed for $N_0 = 10,000$ values and the first $4,000$ ones are dropped in order to free oneself from initial conditions. In a 1-D flow, the wind incidence is constant and so are thus the aerodynamic coefficients; the nonlinearity of the quasi-steady wind loading comes down to the quadratic expression of the relative velocity. For simplicity we consider next a fixed structure in the flow ($x^* = y^* = z^* = \alpha^* = 0$) and define a dimensionless aerodynamic force

$$\mathcal{F} = \frac{F}{\frac{1}{2}\rho C\, B\, U^2} = \frac{\|\mathbf{v}\|^2}{U^2} = 1 + 2\frac{u}{U} + \left(\frac{u}{U}\right)^2. \tag{23}$$

This expression shows the existence of a quadratic term which is usually neglected owing to its (mean-square) smallness; an approximate linear form of this dimensionless loading is thus often adopted

$$\widehat{\mathcal{F}} = 1 + 2\frac{u}{U}. \tag{24}$$

These expressions show that the loading only depends on the dimensionless turbulence u/U, which is characterized by the turbulence intensity

$$I_u = \frac{\sigma_u}{U} \tag{25}$$

chosen equal to $I_u = 20\%$ in the present illustration. The turbulence generated with (22) is thus ultimately normalized by the standard deviation corresponding to this wind intensity. Figure 3-a,b represents samples of $\mathcal{F}$ and $\widehat{\mathcal{F}}$ generated with this procedure. Notice that $\mathcal{F}$ is evidently always positive whereas $\widehat{\mathcal{F}}$ may eventually be negative. Figure 3-c,d represents the histograms of $\mathcal{F}$ and $\widehat{\mathcal{F}}$ as estimates of the probability density functions. They have been obtained as the average histogram of 500 simulations in order to obtain smooth results.

The parabola shape in semi-logarithmic axes indicates a Gaussian distribution for $\widehat{\mathcal{F}}$. On the contrary the semi-logarithmic plot emphasizes the limit $\mathcal{F} > 0$ and illustrates clearly the non Gaussianity of the aerodynamic force. This point is of major concern since both curves tail apart for values larger than 2. The statistics of the extreme values are assessed by simulating 10,000 samples of duration $T = 600s$, storing the maximum and minimum forces obtained on each sample for both aerodynamic expressions, namely m_i , M_i , $\hat{m}_i$ and $\hat{m}_i$, and computing their statistics. Actually, the comparison is rather performed for peak factors defined as

$$\begin{aligned} g_i^+ &= \frac{M_i - \mu_{\mathcal{F}}}{\sigma_{\mathcal{F}}} \quad ; \quad g_i^- = \frac{\mu_{\mathcal{F}} - m_i}{\sigma_{\mathcal{F}}} \\ \hat{g}_i^+ &= \frac{M_i - \mu_{\widehat{\mathcal{F}}}}{\sigma_{\widehat{\mathcal{F}}}} \quad ; \quad \hat{g}_i^- = \frac{\mu_{\widehat{\mathcal{F}}} - m_i}{\sigma_{\widehat{\mathcal{F}}}} \end{aligned} \tag{26}$$

for $i = 1, ..., 10,000$, where $\mu_{\mathcal{F}}$, $\mu_{\widehat{\mathcal{F}}}$, $\sigma_{\mathcal{F}}$ and $\sigma_{\widehat{\mathcal{F}}}$ represent the mean values and standard deviations of the aerodynamic forces. The histograms of the peak factors are represented in Fig. 3-e. We can observe identical distributions for $\hat{g}_i^+$ and $\hat{g}_i^-$ which is due to the probabilistic symmetry of the linearized aerodynamic force. On the contrary, the nonlinear model exhibits different behaviors for values larger and resp. smaller than the mean. It goes with saying that the estimation of design quantities is obviously affected by the "small" quadratic term. This statement is usually disregarded because in a typical statistical analysis, only the mean and standard deviation are considered and they are manifestly not significantly affected by the quadratic term of the loading ($\mu_{\mathcal{F}} \simeq \mu_{\widehat{\mathcal{F}}}$, $\sigma_{\mathcal{F}} \simeq \sigma_{\widehat{\mathcal{F}}}$).

In this illustration the actual peak factor is larger than what would be obtained in the linearized case, because of the presence of only a quadratic term as non Gaussianity catalyst. The linearized case yields therefore to an unsafe design. Opposite situations may also happen where actual extreme values are smaller than those predicted by a linear model; in this case, the design could be more inexpensive, for the same level of safety.

This kind of Monte Carlo illustration is typically not affordable at a design stage. In practical applications the extreme value $\mathcal{F}_{ext}$ of a random process (the aerodynamic force here) is expressed as

$$\mathcal{F}_{ext} = \mu_{\mathcal{F}} + g\,\sigma_{\mathcal{F}} \tag{27}$$

where g is a peak factor obtained from an analytical model. The most famous is certainly due to Rice [28, 29], under assumption of a Gaussian process with independent occurrences of extreme values during the observation window of duration T,

$$g = \sqrt{2\ln \nu_0^+ T} + \frac{\gamma}{\sqrt{2\ln \nu_0^+ T}}, \tag{28}$$

where $\gamma = 0.5772\cdots$ is Euler's constant and ν_0^+ is the zero upcrossing rate, which may be readily deduced from the psd. This universal function is represented in Fig. 4-a, which indicates that typical peak factors for Gaussian processes are in the range $[3; 4]$.

When it comes to extremes of non Gaussian processes, various models exist [30, 31, 32, 33, 34, 35, 36, 37, 38, 39]. Among them, a famous model was developed for cubic

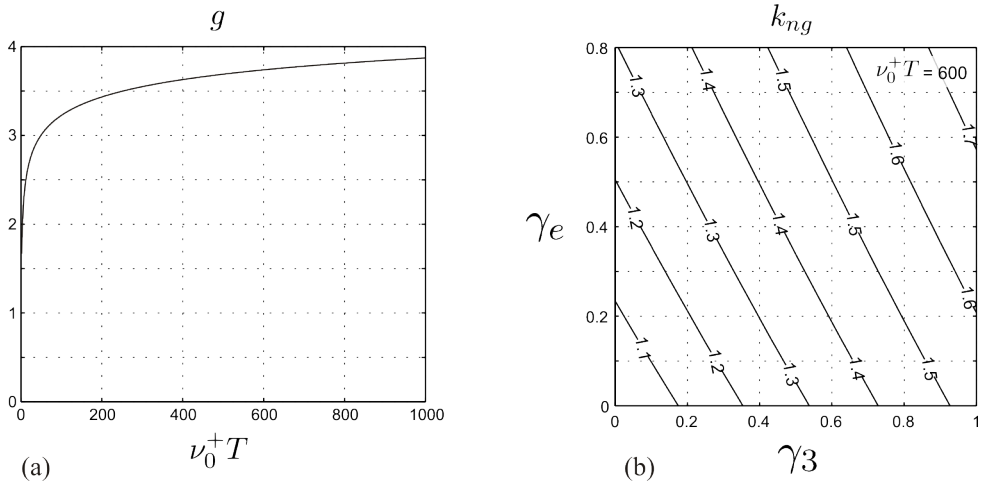

Figure 4. (a) peak factor of a Gaussian process with independent occurrences of extreme values; (b) Multiplicative factor that allows taking into account the non Gaussianity. In this non-Gaussian model, this factor k_{ng} is simply expressed as a function of the skewness γ_3 and excess γ_e coefficients.

transformations of Gaussian processes [40]. It consists in simply estimating the peak factor as

$$g = k_{ng}\left(\sqrt{2\ln\nu_0^+T} + \frac{\gamma}{\sqrt{2\ln\nu_0^+T}}\right), \tag{29}$$

where k_{ng} is a multiplicative factor that takes into account the non-Gaussian nature of the random process. This factor k_{ng} is expressed as a function of the skewness coefficient γ_3, the excess coefficient γ_e and the number of zero upcrossing during the observation period ν_0^+T. It possesses an analytical expression derived from mathematical developments, and is represented in Fig. 4-b for $\nu_0^+T = 600$, a representative order of magnitude in wind engineering applications ($T = 600$s, $\nu_0^+ \simeq 1$Hz). This model suggests that the Gaussian model underestimates extreme values by as much as 30%-50%, which is by the way the order of magnitude of the discrepancy noticed previously with the Monte Carlo illustration.

In the light of this simple extremum model, it appears that the proper estimation of the skewness and eventually excess coefficients of random processes is of paramount importance. Next, we present how these statistical properties of the structural response are computed, and how turbulence characteristics may affect them.

3.3. Non Gaussian structural analysis

The dynamic response of a structure is expressed by means of the equation of motion [41]

$$\mathbf{M}\ddot{\mathbf{x}} + \mathbf{C}\dot{\mathbf{x}} + \mathbf{K}\mathbf{x} = \mathbf{f} \tag{30}$$

which translates the equilibrium of inertial and viscous damping forces, as well as external $\mathbf{f}$ and internal $\mathbf{K}\mathbf{x}$ forces. In a finite element context, $\mathbf{M}$, $\mathbf{C}$ and $\mathbf{K}$ represent the mass,

damping and stiffness matrices while $\mathbf{x}$ represents the nodal displacement of the finite element model and $\mathbf{f}$ collects the forces resulting from the turbulent wind flow around the structure. This equation assumes that the structural behavior is linear.

The first rank stochastic analysis is trivial. It consists in determining the mean response, on the basis of the mean force. After the transient phase vanishes, or under stationary conditions, the mean structural response is simply obtained as

$$\mu_{\mathbf{x}} = \mathbf{K}^{-1}\mu_{\mathbf{f}}. \tag{31}$$

We discuss next the procedure to obtain higher rank properties of the structural response.

If one is interested in the stationary response of the considered structure under a given stationary loading, the Fourier transform of (30) is strictly equivalent and provides a bare insight on the dynamical response. It simply writes [41]

$$\mathbf{X}(\omega) = \mathbf{H}(\omega)\ \mathbf{F}(\omega) \tag{32}$$

where $\mathbf{H}(\omega) = \left(-\mathbf{M}\omega^2 + i\omega\mathbf{C} + \mathbf{K}\right)^{-1}$ is the (complex) transfer function of the system. This formulation is attractive when the applied loading is a random field as the pressures resulting from the turbulent flow. Indeed as show in (32), thanks to structural linearity, every single frequency component may be treated independently from others. Furthermore, the psd of the applied force is expressed as a function of the Fourier transform of the force field, i.e. $\mathbf{F}(\omega)$, by extension of (10). It is then rather straightforward that the psd of the structural response $\mathbf{S}_{\mathbf{x}}(\omega)$ is expressed as

$$\mathbf{S}_{\mathbf{x}}(\omega) = \mathbf{H}(\omega)\,\mathbf{S}_f(\omega)\,\overline{\mathbf{H}^T(\omega)} \tag{33}$$

where $\mathbf{S}_f(\omega)$ is the psd of the loading. Because the aerodynamic force is related to the components of the turbulence by means of the aerodynamic loading model, see e.g. 18, the psd of the loading $\mathbf{S}_f(\omega)$ may be expressed as a function of the psd of the turbulence components. The advantage of the quasi-steady theory is to consider a static transformation from (u, v, w) to the applied forces $\mathbf{f}$. This static transformation is not capable of representing properly the dependency of the wind loading upon the history of the structural motion. For this reason, the psd of the loading is corrected by multiplying, in the frequency domain, the expression obtained from the aerodynamic loading by an admittance function [1, 18, 42]. This function is typically measured in wind tunnel for bluff bodies as civil structures. A deeper discussion on this topic goes beyond the scope of this chapter. We refer to [43, 44] for more information.

Because the psd contains the information necessary to represent the second order statistics of a random process, in particular the variance which is obtained by integration along frequencies as in (11), $\mu_{\mathbf{x}}$ and $\mathbf{S}_{\mathbf{x}}(\omega)$ are sufficient to provide an exhaustive description of the response, provided it is Gaussian, i.e. provided the loading is Gaussian. Traditionally, random structural analysis stops here and analytical peak factors, as given in (28) are called for to determine extreme values.

Nevertheless, we have previously seen that the actual non Gaussian nature of a random process may drastically affect its extreme values. In particular, the non Gaussian random loading resulting from the turbulence, provides a non Gaussian structural response. By

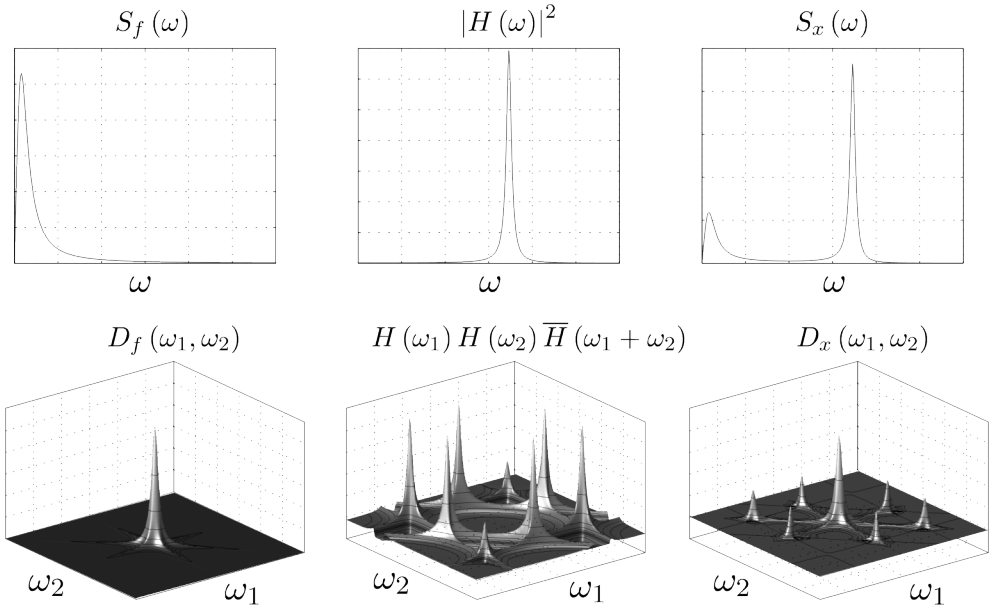

Figure 5. Principle of analysis in the frequency domain. (a) Second order: the psd of the response is obtained by multiplication of the psd of the loading by the squared transfer function $|H(\omega)|^2$; (b) Third order: the bispectrum of the response is obtained by multiplication of the bispectrum of the loading by the Volterra kernel $H(\omega_1)H(\omega_2)\overline{H}(\omega_1+\omega_2)$.

extension of the second rank analysis, the third rank analysis may be regarded as the determination of the bispectrum of the response $\mathbf{D_x}(\omega_1,\omega_2)$ as a function of the bispectrum of the loading $\mathbf{D_f}(\omega_1,\omega_2)$. For instance, in the case of a single degree of freedom system, this relation writes

$$D_x(\omega_1,\omega_2) = H(\omega_1)H(\omega_2)\overline{H}(\omega_1+\omega_2)D_f(\omega_1,\omega_2). \tag{34}$$

It takes a similar but generalized form for multi-degree of freedom systems, see [45]. Because it encapsulates the (first rank) third statistical moment, the bispectrum is strictly sufficient to give a third order probabilistic description of the structural response. Similar developments may be extended to higher orders, with a limitation though due the fact that bi-, tri-, ... spectra require $n-$order multiple integration in order to yield to the n^{th} moment. On account that the functions to be integrated present many zones with large gradients, the computation of such integrals requires a lot of care in the meshing, and are practically not affordable today for $n > 4$.

The principle of analysis in the frequency domain, based on (33)-(34) is illustrated in Fig. 5.

The determination of higher order statistical moments, together with some other information about the band width of the response in the multi-fold frequency spaces, gives access to more appropriate estimates of the peak factors g, by using (29) for instance. As a consequence of the possible dissymmetry, there are typically two estimates of the peak factors and (29) is therefore applied once for values larger than the mean, and a second time for values smaller than the mean.

The analysis method based on (30)-(32) operates in the frequency domain. A similar method, usually referred to as the method of moments, exists in the time domain. In this domain, the stationary solution is obtained as the solution of an algebraic equation, but the method is restricted to a limited class of loading processes, which makes intricate its application to the atmospheric turbulence.

Another analysis method yet is based on Monte Carlo simulations. Samples of the aerodynamic forces are generated and deterministic structural analyses are performed to determine the structural response. An ultimate statistical treatment of the response is performed in order to provide the design values of the response. This method is typically time consuming because it requires a large amount of simulations in order to provide reliable estimates of extreme values. In the framework of a buffeting analysis where the turbulence field (u, v, w) is generated and quasi-steady aerodynamic forces are computed according to the developments of Section 3.1., this Monte Carlo procedure requires to start with the generation of that turbulence field. Nowadays, in the absence of non Gaussian turbulence models, the simulated turbulence field is typically Gaussian [46, 47]. However, generators of non Gaussian random processes exist [48, 49] and they complete the set of necessary tools for consideration of a more realistic turbulence model. Monte Carlo simulations are therefore also receptive to non-Gaussian models of the turbulence.

3.4. Conclusions

Considering reversely the issues raised in this section, we may conclude that (i) structural analysis tools are ready to take on non Gaussian models of wind pressures, which may eventually be obtained as a quasi-steady transformation of the turbulence; (ii) the intrinsic non Gaussianity of the turbulence may therefore be solely integrated; (iii) the linearization of the aerodynamic loading, as usually performed, may yield to drastically over- or under-estimated design quantities; (iv) advanced quasi-steady models generate some non Gaussianity, based on nonlinear static expressions of the turbulence field, but the intrinsic non Gaussianity of the turbulence is not included yet. A precise characterization of the higher statistical properties of the turbulence could be integrated directly into the loading models.

4. Simplified Structural Analysis under Turbulent Flow

We must concede that the rigorous stochastic analysis as based on (33)-(34) is still not commonly applied. Reasons are not only the frustration in front of the lack of knowledge about the non-Gaussianity of wind pressures and turbulence velocities, but also the computational demand of the method. In order to make the analysis method more affordable, several simplified analysis techniques have been proposed. Basing the argument on an illustration obtained with a particular simplified method, the purpose of this section is to show that such methods may also be adapted to include turbulence properties that are not considered today.

For the sake of simplicity, a single degree-of-freedom system is considered with mass, damping and stiffness represented by m, c and k. Consideration of such a system is not really restrictive since the stochastic analysis is anyway performed in a modal basis.

4.1. Second order analysis

Let us come back to the quadratic loading (23). The power spectral density of $\mathcal{F}$ is given as [45]

$$S_{\mathcal{F}}(\omega) = \left(1 + I_u^2\right)^2 \delta(\omega) + \frac{4}{U^2} S_u(\omega) + \frac{2}{U^4} \int_{-\infty}^{+\infty} S_u(\Omega)\, S_u(\Omega - \omega)\, d\Omega \tag{35}$$

whereas the power spectral density of $\widehat{\mathcal{F}}$ is given as

$$S_{\widehat{\mathcal{F}}}(\omega) = \delta(\omega) + \frac{4}{U^2} S_u(\omega). \tag{36}$$

In these expressions, the intensity of the delta-Dirac functions in the first terms represents the squared mean force. For the small turbulence intensities encountered in applications related to atmospheric turbulence, we may agree that the mean force is insensitive to the quadratic term of the loading. The second term provides, after integration along frequencies, a contribution to the variance of order I_u^2 whereas the third term in (35) , which originates from the quadratic term of the aerodynamic loading, provides a contribution of order I_u^4. For this reason, linear and nonlinear loadings are usually considered as equivalent with respect to their variances, and more generally power spectral densities.

The formal application of (33) requires the psd of the response to be computed for many frequencies so that the numerical estimation of its integral provides a precise estimation of the variance of the response. In case of large finite element models, this yields to heavy computational efforts, especially because the estimation of the psd of the force itself may require a huge computational effort . In this connection, approximate solutions are usually chosen. The most famous consists in observing that the natural period of civil structures is one or several orders of magnitude below the characteristic time scale of the atmospheric turbulence. The psd of the response, as computed by (33) on $\omega \in [-\infty; +\infty]$, presents therefore three distinct peaks, corresponding to *background* (1 peak) and *resonant* (2 peaks) components. A fair approximation, apparently suggested by Davenport [50] and later on formally rationalized by Ashraf and Gould, see [51], consists in estimating the variance of the response $\widetilde{m}_{2,x}$ as the sum of two terms corresponding to these components, respectively,

$$\widetilde{m}_{2,x} = \frac{m_{2,f}}{k^2} + \frac{\pi\omega_0}{2\xi} \frac{S_f(\omega_0)}{k^2} \tag{37}$$

where $\omega_0 = \sqrt{k/m}$ is the natural frequency, $\xi = c/2m\omega_0$ is the damping ratio and $m_{2,f}$ is the variance of the aerodynamic force. Notice also that $S_f(\omega) = \left(\frac{1}{2}\rho C\, B\, U^2\right)^2 S_{\mathcal{F}}(\omega)$ according to the scaling chosen above.

Tracing back from (37) to the characteristics of the turbulence, we may see that the variance of the structural response depends essentially on (i) the mean wind velocity U, (ii) the turbulence intensity I_u, (iii) the psd of the wind turbulence around the natural frequency $S_u(\omega_0)$. These issues have been raised for a long time as the predominant features of the statistical properties [50]. Although the psd of the wind turbulence provided by various codes, provisions and standards are not accurately consistent on $S_u(\omega_0)$, everyone at least agrees that these quantities require to be inspected with care in the context of a structural design.

4.2. Third order analysis

The bispectrum of $\mathcal{F}$ is expressed as a function of S_u as a result of the consideration of the nonlinear aerodynamic loading [45]

$$\begin{aligned} B_{\mathcal{F}}(\omega_1,\omega_2) &= \frac{8}{U^4}\left[S_u(\omega_1)S_u(\omega_2)+S_u(\omega_1+\omega_2)S_u(\omega_1)+S_u(\omega_2)S_u(\omega_1+\omega_2)\right] \\ &\quad +\frac{1}{U^6}\int_{-\infty}^{+\infty} S_u(\Omega+\omega_1)S_u(\Omega-\omega_2)S_u(\Omega)\,d\Omega \end{aligned} \tag{38}$$

but under the assumption that u is Gaussian. Because of that, the bispectrum of $\widehat{\mathcal{F}}$ is evidently null,

$$B_{\widehat{\mathcal{F}}}(\omega_1,\omega_2)=0 \tag{39}$$

but if this was not the case, it would simply be proportional to the bispectrum of u, $B_{\widehat{\mathcal{F}}}=\frac{8}{U^3}B_u$, as $S_{\widehat{\mathcal{F}}}(\omega)$ is proportional to $S_u(\omega)$, see (36). In a framework where the non Gaussianity of the wind turbulence would be taken into account, the actual bispectrum of the force (38) should also be complemented by terms in B_u, and there are no reasons yet to postulate that these terms related to the intrinsic non Gaussianity of the turbulence be much smaller or much larger than those resulting from the nonlinearity of the loading.

For reasons similar to those evoked before, the computation of the third moment of the response may turn to a heavy computational task, if (34) has to be twice integrated numerically. Instead, and based on the same assumption of existence of multiple time scales in the response, the third moment of the response $\widetilde{m}_{3,x}$ may be expressed as [52]

$$\widetilde{m}_{3,x}=\frac{m_{3,f}}{k^3}+6\pi\frac{\xi\,\omega_0^3}{k^3}\int_{-\infty}^{+\infty}\frac{B_f(\omega_0,\omega)}{(2\xi\,\omega_0)^2+\omega^2}d\omega. \tag{40}$$

A proper estimation of the third statistical moment of the response is therefore subject to a careful estimation of (i) the third statistical moment of the force $m_{3,f}$ and (ii) the bispectrum of the force $B_f(\omega_1,\omega_2)$ in the vicinity of (ω_1,ω_2)=$(\omega_0,0)$. The first issue is related to the proper identification of the nonlinear transformation from turbulence u to force f on the one hand, and of the possible intrinsic statistical dissymmetry in the turbulence. Concerning the estimation of $B_f(\omega_1,\omega_2)$ in the vicinity of (ω_1,ω_2)=$(\omega_0,0)$, Equation (38) indicates that it is sensitive to $S_u(\omega_0)$ and $S_u(0)$ in the context of this quadratic Gaussian loading. There is no doubt that $B_u(\omega_0,0)$ would also deserve a particular attention if the intrinsic non Gaussianity of the turbulence was considered.

4.3. Further simplification

The practical application of (40) may still be demanding, despite the double integral has been cut down to a single one. A possible way to further simplify the analysis (and that will also highlight the major features of the turbulence that influence the structural response) is to assume that the power spectral density of the turbulence is expressed as

$$S_u(\omega)=\frac{a}{\pi}\frac{\sigma_u^2}{a^2+\omega^2}. \tag{41}$$

where a is a characteristic frequency that needs to be tuned in order to fit the actual data. Various methods exists depending on the desired fitting objective [45, 27]. Substitution of (41) into (35) and (38) and transformation from the dimensionless force $\mathcal{F}$ to the physical one f yield

$$S_f(\omega) = m_{2,f}\frac{a}{\pi}\frac{1}{a^2+\omega^2} \tag{42}$$

$$B_f(\omega) = m_{3,f}\left(\frac{a}{\pi}\right)^2 \frac{a^2+\frac{2}{3}\left(\omega_1^2+\omega_1\omega_2+\omega_2^2\right)}{\left(a^2+\omega_1^2\right)\left(a^2+\omega_2^2\right)\left(a^2+(\omega_1+\omega_2)^2\right)} \tag{43}$$

where the second and third statistical moments of the loading are obtained as

$$m_{2,f} = (\rho C\, B\, U\, \sigma_u)^2 \quad ; \quad m_{3,f} = 3\, I_u\, (\rho C\, B\, U\, \sigma_u)^3\,. \tag{44}$$

Notice that the skewness coefficient of the aerodynamic loading is obtained as

$$\gamma_{3,f} = \frac{m_{3,f}}{(m_{2,f})^{3/2}} = 3I_u. \tag{45}$$

In this context of a 1-D turbulence flow, the pertinence of a third order analysis is therefore directly related to the turbulence intensity.

Substitution of (42) and (43) into (33)-(34) and integration along frequencies provides closed form expressions for the second and third statistical moments of the response. They are written

$$m_{2,x} = m_{3,x}\frac{m_{2,f}}{k^2}\mathcal{A}_2\left(\frac{\omega_0}{a},\xi\right) \quad ; \quad = \frac{m_{3,f}}{k^3}\mathcal{A}_3\left(\frac{\omega_0}{a},\xi\right) \tag{46}$$

where

$$\mathcal{A}_2 = \frac{1}{2\xi}\frac{\frac{\omega_0}{a}\left(1+2\xi\frac{\omega_0}{a}\right)}{1+2\xi\frac{\omega_0}{a}+\left(\frac{\omega_0}{a}\right)^2} \tag{47}$$

$$\mathcal{A}_3 = \frac{\frac{1}{3}\frac{1}{1+8\xi^2}\left(\frac{\omega_0}{a}\right)^2\sum_{k=0}^{k=7}c_k(\xi)\left(\frac{\omega_0}{a}\right)^k}{\left(1+2\xi\frac{\omega_0}{a}\right)\left(1+2\xi\frac{\omega_0}{a}+\left(\frac{\omega_0}{a}\right)^2\right)^2\left(4+4\xi\frac{\omega_0}{a}+\left(\frac{\omega_0}{a}\right)^2\right)\left(1+4\xi\frac{\omega_0}{a}+4\left(\frac{\omega_0}{a}\right)^2\right)} \tag{48}$$

where $c_k(\xi)$, $k=0,...7$, are polynomials in ξ given in Table 1. Because $m_{2,f}/k^2$ and $m_{3,f}/k^3$ are precisely the second and third statistical moments of the response that would be obtained if the response was quasi-static, factors $\mathcal{A}_2$ and $\mathcal{A}_3$ may be seen as the second and third order dynamic amplification factors. They are represented by solid lines in Fig. 6. A major difference between both factors is that the second order one is unbounded for $\xi \to 0$ whereas the third order one is bounded to $\mathcal{A}_3 = 3$.

Finally the non Gaussian peak factor g that is considered for the design requires estimation of the skewness coefficient of the response, expressed as

$$\gamma_{3,x} = \frac{m_{3,x}}{m_{2,x}^{3/2}} = \frac{\mathcal{A}_3\, m_{3,f}}{(\mathcal{A}_2\, m_{2,f})^{3/2}} = \frac{\mathcal{A}_3}{\mathcal{A}_2^{3/2}}\gamma_{3,f}. \tag{49}$$

k	$c_k\left(\xi\right)$
0	32
1	352
2	$8\left(17+184\xi^2\right)$
3	$16\xi\left(53+184\xi^2\right)$
4	$131+2040\xi^2+2816\xi^4$
5	$2\left(197+1128\xi^2+512\xi^4\right)$
6	$12\left(3+34\xi^2+80\xi^4\right)$
7	$24\xi\left(1+8\xi^2\right)$

Table 1. Coefficients c_k for the computation of the third order dynamic amplification coefficient, (48).

The ratio $\mathcal{A}_{\gamma_3} = \mathcal{A}_3/\mathcal{A}_2^{3/2}$ appears therefore to be the scalar that characterizes the decrease of skewness from the loading to the response. As a consequence of the central limit theorem, it is expected that a structure responds in such a way that it is more Gaussian than the loading to which it is subjected (because the structural response is obtained by convolution). It is thus expected that $\mathcal{A}_{\gamma_3}$ be smaller than unity. Moreover, $\mathcal{A}_{\gamma_3}$ is a function of only ξ and ω_0/a, i.e. the structural parameters, once a has been fixed. One can readily check that the limit behaviors of $\mathcal{A}_2$ and $\mathcal{A}_3$ corresponds to a quasi-static response for a highly damped structure ($\mathcal{A}_2 \simeq 1$ for $\frac{a}{\omega_0} \ll \xi \ll 1$; $\mathcal{A}_3 \simeq 1$ for $1 \lesssim \xi$) and to a dynamic response for a slightly damped structure ($\mathcal{A}_2 \simeq 1/2\xi$ for $\xi \ll \frac{a}{\omega_0}$; $\mathcal{A}_3 \simeq 3$ for $\xi \ll 1$). These limit cases translate into asymptotic behaviors $\mathcal{A}_{\gamma_3} \simeq 1$ for quasi-static response ($\xi \ll 1$), and $\mathcal{A}_{\gamma_3} \simeq \xi^{3/2}$ for a dynamic response ($\xi \gg 1$). The most basic and typical shape of $\mathcal{A}_{\gamma_3}\left(\xi\right)$ is therefore monotonic, increasing from 0 to 1. This function is reported in Fig. 6, for the particular psd of turbulence given in (41). Consideration of variants of the previously assumed power spectral density (41) shows that $\mathcal{A}_{\gamma_3}$ is little sensitive to that assumed frequency distribution. It is however much more sensitive to the nonlinearity of the aerodynamic force.

Similar developments exist for the fourth order analysis and yield a scalar $\mathcal{A}_{\gamma_4}$ that similarly represents the reduction of the excess coefficient trough the process of the dynamic response. It turns out [45] that this other coefficient is almost equal to $\mathcal{A}_{\gamma_3}$. It is not further discussed here.

As a conclusion, this design procedure presented in this section indicates that the skewness of the response is smaller than the skewness of the loading. This latter one may therefore be considered as a safe estimate of the skewness of the response ($\mathcal{A}_{\gamma_3} \simeq 1$). This highlights again the need to precisely estimate the statistical properties of the aerodynamic loads applied on a structure. Furthermore, if the shaping parameter a may be estimated from the actual loading, the abacus given in Fig. 6 allows a more precise estimation of $\mathcal{A}_{\gamma_3}$, and therefore the skewness of the response $\gamma_{x,3}$, thanks to (49).

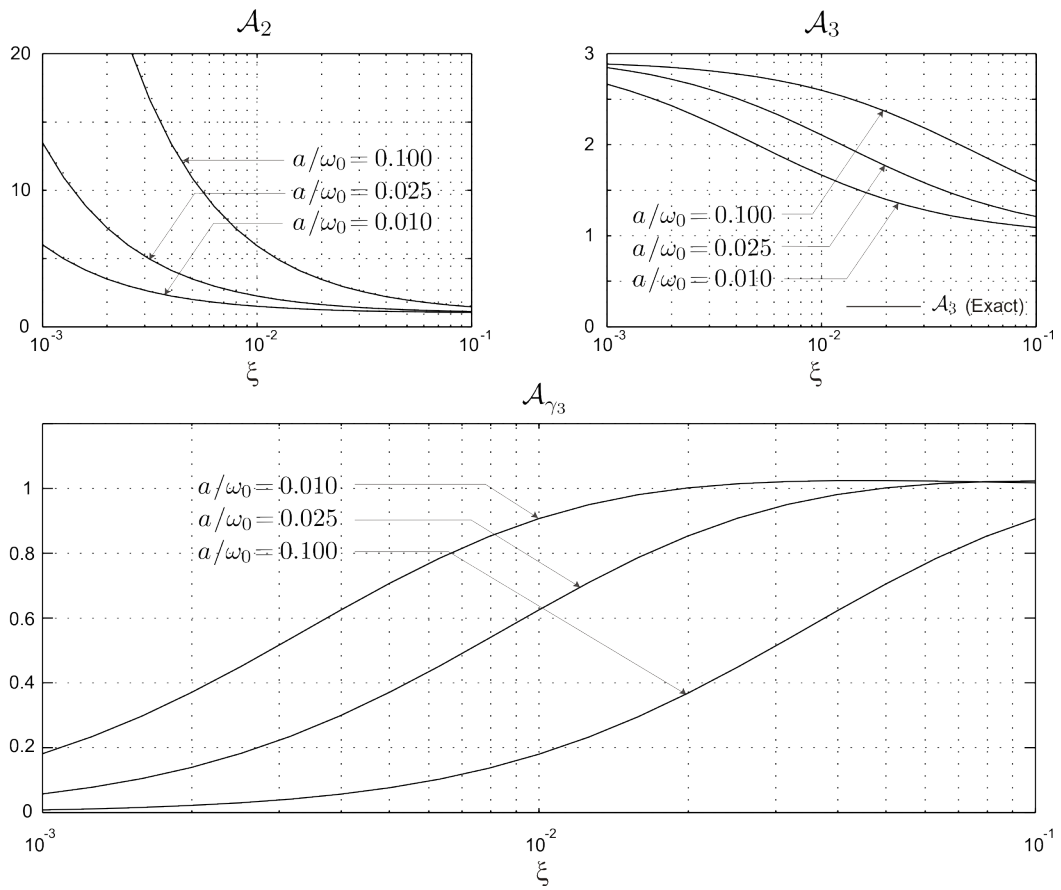

Figure 6. Dynamic amplification factors $\mathcal{A}_2$ and $\mathcal{A}_3$ of the second and third statistical moment of the response. The second moment grows up to infinity for $\xi \to 0$, whereas the third moment is limited to three times its quasi-static values. The lower plot represents $\mathcal{A}_{\gamma_3}$, the coefficient by which the skewness of the force is reduced to obtain the skewness coefficient of the structural response.

5. Focus on the statistical properties of forces generated by turbulence

Along the same line as the conclusions of the previous section, and with the firm wish to point out the statistical properties of the atmospheric turbulence that need to be considered the most carefully, there is evidence that the statistical properties of the loading requires a deeper investigation. To this aim, we come back in this section to a more general case, where the 2-D wind flow around a structure with nonlinear aerodynamic coefficients is investigated. More precisely, we consider the most general nonlinear quasi-steady loading given by (18)-(21), but limit the turbulence field to two components ($v = 0$). This is motivated by the fact that the structural motion takes place in a space of dimension smaller than or equal to 2, e.g. along a line for a roof with a proper bracing system (dimension 1), in a vertical plane for a bridge deck (dimension 2), in a horizontal plane for a high-rise building (dimension 2). It is often admitted that the small surface roughness and the large structural rigidity along the third direction do not allow for a significant motion, which therefore justifies the focus on a 2-D wind flow.

5.1. 2-D turbulence model

Plugging (19)-(21) into (18), one obtains

$$\frac{F}{\frac{1}{2}\rho\, B\, U^2} = \left[\sum_{k=0}^{p} c_k \left(\arctan \frac{w - z^*}{U + u - x^*}\right)^k\right] \left[\left(1 + \frac{u - x^*}{U}\right)^2 + \left(\frac{w - z^*}{U}\right)^2\right]. \quad (50)$$

In the following, we consider one aerodynamic force at a time and F may therefore refer to drag as well as moment or lift forces.

The subtraction of x^* and z^* from the corresponding components of turbulence corresponds to considering the relative wind velocity. This is a simple way to introduce in the model the aeroelastic effects (fluid-structure interaction), which is valid as long as the quasi-steady assumption holds, i.e. as long as the considered reduced frequencies of the motion are small. In the linearized aerodynamic model, this materializes by a supplementary damping. This damping may be positive or negative depending on c_1, the derivative of the aerodynamic coefficient with respect the angle of attack. Positive damping is of course welcome, whereas negative damping may lead to troublesome situations when it compensates for the structural damping [1].

Even if $x^*/U \ll 1$ and $z^*/U \ll 1$, the formal neglect of x^* and z^* is a crude assumption that does not allow for instance the modeling of the supplementary damping in the linearized aerodynamic loading. In the context of the nonlinear model (50), x^*/U and z^*/U are indeed much smaller than unity but they are responsible for the existence of a nonlinear damping, slight indeed, but sufficient to drive the dynamic response of the structure to that of a nonlinear system. It is well known [53] that systems presenting a nonlinear damping even slight exhibit a dynamic response that is significantly different from that of a linear system. This particular case is not discussed further here as the main scope concerns the characteristics of the turbulence. From (50) we thus drop terms in x^* and z^* and express

the dimensionless aerodynamic force as

$$\mathcal{F} = \frac{F}{\frac{1}{2}\rho\, B\, U^2} = \left[\sum_{k=0}^{p} c_k \left(\arctan\frac{\hat{w}}{1+\hat{u}}\right)^k\right]\left[(1+\hat{u})^2+\hat{w}^2\right] \tag{51}$$

where $\hat{u} = u/U$ and $\hat{w} = w/U$ are the dimensionless turbulence components. In the context of this 2-D turbulence field, the linearized aerodynamic force is readily obtained as

$$\widetilde{\mathcal{F}} = c_0 + 2c_0\hat{u} + c_1\hat{w}. \tag{52}$$

The statistical properties of $\mathcal{F}$ are exhaustively expressed by its probability density function $p_{\mathcal{F}}(\mathcal{F})$ (pdf), which may be estimated, from the (known) joint probability density function $p_{\hat{u}\hat{w}}$ of $\hat{u}$ and $\hat{w}$, as

$$p_{\mathcal{F}}(\mathcal{F}) = \lim_{d\mathcal{F}\to 0}\frac{1}{d\mathcal{F}}\iint_{\mathcal{F}<\mathcal{F}(\hat{u},\hat{w})<\mathcal{F}+d\mathcal{F}} p_{\hat{u}\hat{w}}(\hat{u},\hat{w})d\hat{u}d\hat{w}. \tag{53}$$

The complexity of (51) does not allow however to express $p_{\mathcal{F}}(\mathcal{F})$ explicitly. A possible solution to cope with this problem is to limit the statistical description of $\mathcal{F}$ to its statistical moments. In particular, raw moments are defined as

$$\mu_{\mathcal{F},k} \;=\; E\left[\mathcal{F}^k\right] \quad \text{for } k = 1,\ldots,+\infty \tag{54}$$

where $E[\,]$ represents the mathematical expectation operator. Although an infinite number of moments is in principle necessary to represent exhaustively the random variable $\mathcal{F}$, its representation is usually limited to the first few moments (typically up to $\mu_{\mathcal{F},4}$). Their exact expressions may be obtained analytically but yields excessively long formulations. In order to circumvent this problem, the asymptotic statistical moments obtained for small turbulence intensities, $I_u, I_w \ll 1$ may be obtained [54]. For instance, for $p = 2$ (quadratic aerodynamic coefficient),

$$\mu_{\mathcal{F},1} \;\simeq\; c_0\left(1+I_u^2+I_w^2\right) + I_uI_w\rho c_1\left(1-2I_w^2\right) + \frac{I_w^2}{2}c_2\left(1+I_w^2\right) \tag{55}$$

$$\begin{aligned}\mu_{\mathcal{F},2} \;\simeq\;& c_0^2\left(1+6I_u^2+2I_w^2\right) + c_1^2I_w^2\left(1+\left(1+2\rho^2\right)I_u^2+4I_w^2\right)\\ &+c_0c_2I_w^2\left(1+\left(1+2\rho^2\right)I_u^2+4I_w^2\right) + c_2^2I_w^4\left(\frac{3}{4}+\frac{5I_w^2}{2}\right)\\ &+c_0c_1I_uI_w\rho\left(6+6I_u^2+10I_w^2\right) + c_1c_2I_uI_w^3\rho\left(3-15I_w^2\right)\end{aligned} \tag{56}$$

$$\begin{aligned}\mu_{\mathcal{F},3} \;\simeq\;& c_0^3\left(1+15I_u^2+3I_w^2\right) + c_1^3\rho I_uI_w^3\left(9+3\left(3+2\rho^2\right)I_u^2+30I_w^2\right)\\ &+c_2^3\frac{15I_w^6}{8}\left(1+7I_w^8\right) + c_0^2c_1I_uI_w\rho\left(15+90I_u^2+72I_w^2\right) + \frac{3I_w^4}{2}c_0^2c_2\\ &+c_0^2c_2I_w^2\left(\frac{3I_w^2}{2}+\left(1+2\rho^2\right)9I_u^2+\frac{21I_w^2}{2}\right) + c_1^2c_2I_w^4\left(\frac{9}{2}+\frac{75I_w^2}{2}\right)\\ &+\frac{9}{2}\left(1+4\rho^2\right)I_u^2I_w^4c_1^2c_2 + 3c_0c_1^2I_w^2\left(1+6\left(1+2\rho^2\right)I_u^2+7I_w^2\right)\\ &+c_0c_2^2I_w^4\left(\frac{9}{4}+\frac{9}{4}\left(1+4\rho^2\right)I_u^2+\frac{75I_w^2}{4}\right) + c_1c_2^2I_uI_w^5\rho\left(\frac{45}{4}-105I_w^2\right)\\ &+c_0c_1c_2I_uI_w^3\rho\left(27+9\left(3+2\rho^2\right)I_u^2+90I_w^2\right).\end{aligned} \tag{57}$$

These expressions are obtained regardless of the relative magnitude of c_0, c_1 and c_2 and could eventually be further simplified if one of them was much smaller than the other ones.

Similar but simpler developments for the linearized aerodynamic force gives

$$\begin{aligned} \mu_{\widetilde{\mathcal{F}},1} &= c_0 \\ \mu_{\widetilde{\mathcal{F}},2} &= c_0^2\left(1+4I_u^2\right)+c_1^2I_w^2+4c_0c_1\rho I_u I_w \\ \mu_{\widetilde{\mathcal{F}},3} &= 0 \end{aligned} \tag{58}$$

The particular shape of aerodynamic coefficients for bridge decks is such that c_0 is typically of order 1, c_1 too -except for lift forces that may show a stronger dependence to the angle of attack, up to $c_1 = O(10)$-, whereas c_2 is typically of order 10. Also based on the fact that the turbulence intensities I_u and I_w lie within the range $[0;\ 0.20]$ depending on the roughness of the surrounding terrain, one may conclude from (55)-(56) that the linear model captures fairly well the most important terms necessary for a decent estimation of the mean and standard deviation of the aerodynamic force. Other terms, i.e. those present in (55)-(56) but not (58) are indeed of a smaller order of magnitude for this kind of application (notice they may however become predominant for other applications). This explains why, in the framework of the second order analyses performed during the last decades, linear loading models were esteemed so much.

Nevertheless, the linear model is of course incapable of representing properly the third and higher statistical moments of the loading, unlike the nonlinear model. Without a precise information about the relative importance of c_0, c_1, c_2 and eventually higher derivatives of the aerodynamic coefficient, it is difficult to dig into the series of terms in (57) to take out, in a general fashion, the dominant contributions. However, in practical applications, it appears that the curvature c_2 and the intensity of the transverse turbulence I_w are responsible for significantly skewed distributions of the loading.

Formulae (55)-(57) refer to a quadratic aerodynamic coefficient; a general procedure is presented in [54] to obtain similar expressions for any higher degree polynomial approximation. Application of such awkward relations may appear odd at first sight, especially because Monte Carlo simulations may provide similar results, and even without having to formulate the assumptions of small turbulence intensities. They consists in computing the statistical moments of $\mathcal{F}$, integrals of $p_{\mathcal{F}}(\mathcal{F})$, see (53), from a proper sampling in the high-dimensional $(\hat{u}, \hat{w}, \mathcal{F})$ space. This method is really powerful but its crude application is known to be excessively time consuming, a reason for which approximate formula as (55)-(57) are useful.

5.2. Example

A brief example is presented next in order to illustrate the influence of the turbulence on statistical properties of the nonlinear aerodynamic loading. To this purpose, the drag coefficient of the new Tacoma Narrows bridge is considered [1], see Fig. 7-a. It exhibits a typical bowl-shape which indicates that the drag force is roughly constant for small wind incidences (usually due to a high deck thickness and a flat vertical wall to the wind). The slight typical dissymmetry for larger wind incidences is a due to the dissymmetry of the

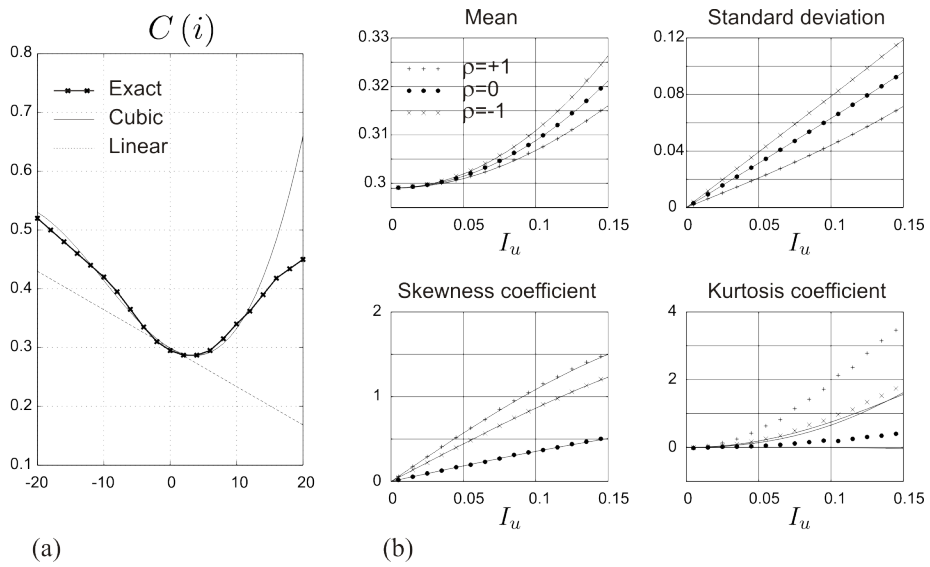

Figure 7. (a) Drag coefficient of the new Tacoma-Narrows bridge project, as a function of the wind incidence i; (b) Mean, standard deviation, skewness and kurtosis of the cubic aerodynamic force, as a function of the turbulence intensity I_u, with $I_w = I_u/2$ and for various correlation coefficients between u and w.

cross sectional profile about a horizontal axis, an unavoidable consequence of the necessity to present a flat circulation surface. The limitation of the traditional linear loading model is illustrated by the representation of the linear approximation of the drag coefficient, which clearly underestimates the actual drag force. On the contrary, the third degree polynomial approximation (which is considered next) provides an accurate fitting to the actual drag coefficient. This fitting is based on a stochastic linearization principle considering the probabilistic character of the range of variation of the wind incidence, see [26], (based here on $I_u = 0.1$; $I_w = 0.05$ and $\rho = 0.5$) and yields

$$c_0 = 0.299; \quad c_1 = -0.375; \quad c_2 = 2.43; \quad c_3 = 4.60. \tag{59}$$

The first four statistical characteristics (mean, standard deviation, skewness coefficient, excess coefficient) are obtained from the raw moments. They are represented for the considered drag force in Fig. 7-b, as a function of the turbulence intensity I_u, with $I_w = I_u/2$ and for various correlation coefficients ρ between u and w. We may observe that the mean aerodynamic force is relatively few affected by the nonlinearity of the loading, even by the turbulence intensity. Moreover, the standard deviation of the force seems to depend linearly on the turbulence intensity, which is also predicted by the linear model. Actually there is so to say no discrepancy between the standard deviations obtained with the linear and cubic loading models. The linear model is therefore sufficient for the representation of the first and second order statistics of the loading.

Plots corresponding to the third and fourth moments indicate that the skewness and kurtosis coefficient of this loading may be large enough to significantly affect the statistics of the extreme values of the force. The results represented by symbols are obtained with a

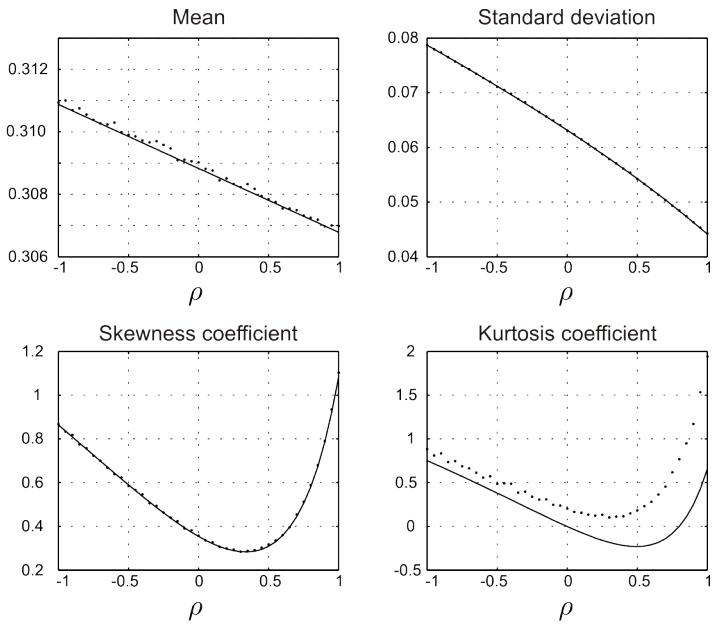

Figure 8. Influence of the correlation between turbulence components, on the first four statistical characteristics of the drag coefficient of the new Tacoma-Narrows bridge deck (for $I_u = 0.1$ and $I_w = 0.05$).

Monte Carlo simulation (generation of 500,000 samples of the turbulence and computation of the wind forces for each of them), whereas the continuous lines correspond to the analytical approximations obtained for small turbulence intensity. These expressions provide a very good approximation up to the third order, for any correlation between the turbulence components u and w. Figure 7-b also shows that the skewness and kurtosis of the loading are highly sensitive to the correlation ρ between turbulence components: for the particular case of the new Tacoma-Narrows bridge, an inappropriate choice of ρ may result in more than 100% discrepancy on the estimation of the skewness coefficient.

This high sensitivity to this correlation coefficient is emphasized in Fig. 8, where the first four statistical characteristics are represented as a function of the correlation between the turbulence components. This graph is obtained for $I_u = 0.1$ and $I_w = 0.05$. On this figure, we may observe the strong influence of ρ on the standard deviation; this kind of result should encourage any designer to precisely assess the actual correlation between turbulence components. The dependency of the skewness and kurtosis upon the correlation ρ is not monotonic and presents large gradients. This further illustrates the need to better estimate the correlation between turbulence components. Notice that the approximate relations (solid lines) matches properly the results of the Monte Carlo simulation (dots), except for the kurtosis for which only the global profile is correctly captured.

-

5.3. Outlook

In this section we have presented simplified expressions for the computation of the statistical properties of the nonlinear aerodynamic loading. They are based on the assumption that the joint distribution representing the statistics of the components u and w of the turbulence are jointly Gaussian. In this context, we have shown the high sensitivity of the skewness and kurtosis of the aerodynamic loading to the correlation between u and w. According to the developments of the former Section, this sensitivity of the loading translates automatically into a significant sensitivity of the structural response.

This strong dependence to the correlation between turbulence components suggests that the joint distribution between u and w be estimated accurately. In particular, there are no reasons for the marginal distributions of u and w (separately) to be Gaussian, and this appears to be a first topic that needs to be refined in the future. As a potential outlook, similar expressions could then be developed (or Monte Carlo simulations could be performed) in the context of a more realistic first-rank turbulence characteristics. They would in turn provide more accurate estimates of the structural response to turbulent loading.

6. Conclusions

Throughout this chapter we have pinpointed a series of statistical characteristics of the turbulence that would need to be assessed more precisely in order to properly feed advanced aerodynamic loading models. They are summarized in this section.

Regarding the traditional linearized aerodynamic loading model, the current characterization of the turbulence is obviously sufficient as it has been being applied for more than fifty year, but conceding however that the relative importance of the correlation between different components of the turbulence plays a significant role -as shown in Section 5.2.- that is probably too often disregarded.

First rank properties of the turbulence that would require to be precisely estimated may be grouped into two sets: unilateral properties and those related to crossed statistics. Indeed, in a non Gaussian framework, the mean and standard deviation of each turbulence components are no longer sufficient to fully describe them. Realistically third and fourth statistical moments could be obtained and although they do not exhaustively complete the statistical representation, they would already provide a novel insight onto the matter. Besides, the joint distributions between the components of turbulence would also require a particular attention. This is parallel to the enhancement of the marginal distributions. Conforming to the significant sensitivity to the correlation between turbulence components, as illustrated in the former example, it is evident that these joint distributions require a particular attention too.

Second rank properties of the turbulence that deserve attention may also be grouped into two similar sets. On the one hand, unilateral power spectral densities available today are typically sufficient to allow a second order analysis. As shown by the background/resonant decomposition, the second order structural response is mainly dependent on (i) the variance of the loading (a first rank property) and (ii) the ordinate, at the natural frequency, of power spectral densities of applied loads, and therefore of the components of the turbulence. Because many models are available to model the power spectral density of turbulence, which

may significantly differ from each other in the high frequency range, a precise second order analysis is typically achieved by selecting the proper power spectral density of turbulence. We have also seen in Section 4.2. that the third order structural response mainly depends on the particular shape of the bispectrum of the force in the vicinity of $(\omega_1, \omega_2) = (\omega_0, 0)$, which therefore involves $S_u(\omega_0)$ and $S_u(0)$ because of the quadratic term(s) in turbulence components. This indicates that an accurate estimation of the low frequency content of the turbulence, by means of $S_u(0)$, is also a key issue that will allow premium structural analyses. On the other hand, crossed probabilities between two different turbulence components or between the same component but at different locations in space, play also an important role, especially when the analysis of large structures spread out along several hundreds of meters is in question. This latter case was not really discussed in this chapter, but we may at least bring back again the necessity to properly model the correlation between various turbulence components.

Third rank properties of the turbulence need of course to be modeled properly for a sound application of a third order structural analysis. No notorious model seem to exist to hand yet in this picture, despite some observations and acknowledgment that the wind turbulence is non Gaussian. The full third order description of the turbulence may therefore be regarded as a must. Again, bispectrum of each turbulence component as well as cross-bispectra between various components and/or at various locations in space need to be assessed. Notice that the distinction "and/or" is made here, because up to three different random processes may be considered for the estimation of a cross-bispectrum. We must concede that the full third rank description of the turbulence is a utopian aim. It could eventually be brought down taking into account that essentially the bispectrum of the force around $(\omega_1, \omega_2) = (\omega_0, 0)$ require to be accurately estimated.

Fourth and higher rank properties of the turbulence components may also be provided in the same way, but there are few hopes that these quantities be uniformly standardized in a near future.

Structural analysis tools, as the frequency domain analysis or Monte Carlo simulations, are now ready to incorporate the third and higher rank properties of the wind forces. In this connection, wind forces are estimated from pressures, which are themselves expressed as a function of the turbulence components, thanks to the nonlinear aerodynamic model considered in this chapter. As a matter of fact, it is obvious that bypassing the description of the turbulence in favor of a complete non-Gaussian model of the wind pressures would provide an even more realistic model, since the developments do not rest then on a theoretical aerodynamic model. In other words, if one had a precise probabilistic description of the pressures along the structure under investigation, the estimation of the corresponding forces would naturally sound more realistic. Nevertheless, to utilize wind pressures instead of turbulence velocity is still restricted to applications where wind-tunnel experiments or advanced CFD computations are performed. On the contrary, an aerodynamic model based on a statistical description of the turbulence is applicable to a wide range of applications and seems therefore to be the perfect canvas for standardization.

References

[1] E. Simiu and R. Scanlan. *Wind Effects On Structures*. John Wiley and Sons, 3rd edition, 1996.

[2] A. Larsen. *Aerodynamics of Large Bridges*. Balkema, Amsterdam, 1992.

[3] C. Dyrbye and S. O. Hansen. *Wind loads on structures*. 1997.

[4] H. W. Liepmann. On the application of statistical concepts to the buffeting problem. *Journal of Aeronautical Sciences*, 19(12):793–800, 1952.

[5] C. G. Bucher and Y. K. Lin. Effects of wind turbulence on motion stability of long-span bridges. *Journal Of Wind Engineering And Industrial Aerodynamics*, 36(1-3):1355–1364, 1990. Times Cited: 2 2.

[6] A. Jain, N. P. Jones, and R. H. Scanlan. Coupled flutter and buffeting analysis of long-span bridges. *Journal Of Structural Engineering-Asce*, 122(7):716–725, 1996. Times Cited: 57.

[7] H. Katsuchi, N. P. Jones, R. H. Scanlan, and H. Akiyama. Multi-mode flutter and buffeting analysis of the akashi-kaikyo bridge. *Journal Of Wind Engineering And Industrial Aerodynamics*, 77-8:431–441, 1998. Times Cited: 12.

[8] G. Solari and G. Piccardo. Probabilistic 3-d turbulence modeling for gust buffeting of structures. *Probabilistic Engineering Mechanics*, 16(1):73–86, 2001. doi: DOI: 10.1016/S0266-8920(00)00010-2.

[9] M. Di Paola, G. Ricciardi, and M. Vasta. A method for the probabilistic analysis of nonlinear systems. *Probabilistic Engineering Mechanics*, 10(1):1–10, 1995. Times Cited: 7.

[10] M. Grigoriu and S. T. Ariaratnam. Response of linear systems to polynomials of gaussian processes. *Transactions of the ASME. Journal of Applied Mechanics|Transactions of the ASME. Journal of Applied Mechanics*, 55(4):905–10, 1988. Times Cited: 0.

[11] Keh-Shin Lii. Nonlinear systems and higher-order statistics with applications. *Signal Processing*, 53(2-3):165–177, 1996.

[12] X. J. Zhang, H. F. Xiang, and B. N. Sun. Nonlinear aerostatic and aerodynamic analysis of long-span suspension bridges considering wind-structure interactions. *Journal Of Wind Engineering And Industrial Aerodynamics*, 90(9):1065–1080, 2002. Times Cited: 14.

[13] M. T. Chay, R. Wilson, and F. Albermani. Gust occurrence in simulated non-stationary winds. *Journal Of Wind Engineering And Industrial Aerodynamics*, 96(10-11):2161–2172, 2008.

[14] L. Chen and C. W. Letchford. Numerical simulation of extreme winds from thunderstorm downbursts. *Journal Of Wind Engineering And Industrial Aerodynamics*, 95(9-11):977–990, 2007. doi: DOI: 10.1016/j.jweia.2007.01.021.

[15] A. Kareem and T. Kijewski. Time-frequency analysis of wind effects on structures. *Journal Of Wind Engineering And Industrial Aerodynamics*, 90(12-15):1435–1452, 2002. Times Cited: 9.

[16] P. D. Spanos, A. Sofi, and M. Di Paola. Nonstationary response envelope probability densities of nonlinear oscillators. *Journal Of Applied Mechanics-Transactions Of The Asme*, 74(2):315–324, 2007. Times Cited: 0.

[17] A. Preumont. *Random Vibration and Spectral Analysis*. Kluwer Academic Publishers, 1994.

[18] J. D. Holmes. *Wind Loading on Structures*. SponPress, London, 2nd edition edition, 2007.

[19] A. Papoulis. *Probability, Random Variables, and Stochastic Processes*. McGraw Hill, New York, 1965.

[20] Arkady Tsinober. *A conceptual introduction to turbulence*. Fluid Mechanics and its Applications. Springer, Dodrecht, 2009.

[21] ESDU. *Characteristics of atmospheric turbulence near ground. Part II: single point data for strong winds (neutral atmosphere)*. Engineering Sciences Data Unit, London, 1993.

[22] J. Hojstrup, K.S. Hansen, B. J. Pedersen, and M. Nielson. Non gaussian turbulence, 1-5 March 1999 1999.

[23] J. G. Jones. Measured statistics of multicomponent gust patterns in atmospheric turbulence. *Journal Of Aircraft*, 44:1559–1567, 2007. Times Cited: 0.

[24] Yi Li and Charles Meneveau. Origin of non-gaussian statistics in hydrodynamic turbulence. *Physical Review Letters*, 95(16):164502, 2005. Copyright (C) 2010 The American Physical Society Please report any problems to prola@aps.org PRL.

[25] S. H. Seong and J. A. Peterka. Experiments on fourier phases for synthesis of non-gaussian spikes in turbulence time series. *Journal Of Wind Engineering And Industrial Aerodynamics*, 89(5):421–443, 2001.

[26] V. Denoël. Polynomial approximation of aerodynamic coefficients based on the statistical description of the wind incidence. *Probabilistic Engineering Mechanics*, 24(2):179–189, 2009. doi: DOI: 10.1016/j.probengmech.2008.05.002.

[27] C. Floris. Equivalent gaussian process in stochastic dynamics with application to along-wind response of structures. *International Journal Of Non-Linear Mechanics*, 31(5):779–794, 1996. Times Cited: 6.

[28] Zakhar Kabluchko. Extremes of space-time gaussian processes. *Stochastic Processes And Their Applications*, 119(11):3962–3980, 2009.

[29] S. O. Rice. Mathematical analysis of random noise. *Bell System Technical Journal*, 24:46–156, 1945.

[30] Ross B. Corotis, Anne M. Dougherty, and Wei Xu. Extreme value index and tail probability estimates for mixed distributions. *Probabilistic Engineering Mechanics*, 23(4):385–392, 2008.

[31] M. Gioffre and V. Gusella. Peak response of a nonlinear beam. *Journal Of Engineering Mechanics-Asce*, 133(9):963–969, 2007. 0733-9399.

[32] S. Gupta and P. van Gelder. Extreme value distributions for nonlinear transformations of vector gaussian processes. *Probabilistic Engineering Mechanics*, 22(2):136–149, 2007. 0266-8920.

[33] T. Jakubowski. The estimates of the mean first exit time from a ball for the alpha-stable ornstein-uhlenbeck processes. *Stochastic Processes And Their Applications*, 117:1540–1560, 2007. Times Cited: 0.

[34] A. Kareem and Y. Zhou. Gust loading factor - past, present and future. *Journal Of Wind Engineering And Industrial Aerodynamics*, 91(12-15):1301–1328, 2003. Sp. Iss. SI.

[35] M. Kasperski. Extreme wind load distributions for linear and nonlinear design. *Engineering Structures*, 14(1):27–34, 1992.

[36] B. J. Leira. Extremes of gaussian and non-gaussian vector processes: a geometric approach. *Structural Safety*, 25(4):401–422, 2003. Times Cited: 3.

[37] A. Naess. Crossing rate statistics of quadratic transformations of gaussian processes. *Probabilistic Engineering Mechanics*, 16(3):209–217, 2001. Times Cited: 11.

[38] Ulrik Dam Nielsen. Calculation of mean outcrossing rates of non-gaussian processes with stochastic input parameters – reliability of containers stowed on ships in severe sea. *Probabilistic Engineering Mechanics*, 25(2):206–217, 2010.

[39] Krzysztof Podgorski and Igor Rychlik. Envelope crossing distributions for gaussian fields. *Probabilistic Engineering Mechanics*, 23(4):364–377, 2008.

[40] K. R. Gurley, M. A. Tognarelli, and A. Kareem. Analysis and simulation tools for wind engineering. *Probabilistic Engineering Mechanics*, 12(1):9–31, 1997. Times Cited: 21.

[41] R. W. Clough and J. Penzien. *Dynamics of structures*. McGraw-Hill, New-York, 2nd edition edition, 1993.

[42] F. Tubino. Relationships among aerodynamic admittance functions, flutter derivatives and static coefficients for long-span bridges. *Journal Of Wind Engineering And Industrial Aerodynamics*, 93(12):929–950, 2005.

[43] G. Diana, S. Bruni, A. Cigada, and E. Zappa. Complex aerodynamic admittance function role in buffeting response of a bridge deck. *Journal Of Wind Engineering And Industrial Aerodynamics*, 90(12-15):2057–2072, 2002. Times Cited: 4.

[44] R. H. Scanlan and N. P. Jones. A form of aerodynamic admittance for use in bridge aeroelastic analysis. *Journal Of Fluids And Structures*, 13(7-8):1017–1027, 1999. Times Cited: 10.

[45] V. Denoël. *Application of stochastic analysis methods to the study of the effects of wind on civil engineering structures*. PhD thesis, 2005.

[46] L. Carassale and G. Solari. Monte carlo simulation of wind velocity fields on complex structures. *Journal Of Wind Engineering And Industrial Aerodynamics*, 94(5):323–339, 2006. Times Cited: 3.

[47] M. Di Paola. Digital simulation of wind field velocity. *Journal Of Wind Engineering And Industrial Aerodynamics*, 74-6:91–109, 1998. Times Cited: 25 2nd European and African Conference on Wind Engineering JUN 22-26, 1997 GENOA, ITALY.

[48] G. Bartoli, C. Borri, and L. Facchini. Simulation of non-gaussian wind pressures on a 3-d bluff body and estimation of design loads. *Computers and Structures*, 80(12):1061–1070, 2002. Times Cited: 0.

[49] K. K. Phoon, S. T. Quek, and H. W. Huang. Simulation of non-gaussian processes using fractile correlation. *Probabilistic Engineering Mechanics*, 19(4):287–292, 2004. Times Cited: 4.

[50] A. G. Davenport. Buffeting of a suspension bridge by storm winds. *Journal of the Structural Division ASCE*, (88):233–264, 1962.

[51] M. Ashraf Ali and P. L. Gould. On the resonant component of the response of single degree-of-freedom systems under random loading. *Engineering Structures*, 7(4):280–282, 1985.

[52] V. Denoël. On the background and biresonant components of the random response of single degree-of-freedom systems under non-gaussian random loading. *(under submission)*.

[53] H. K. Khalil. *Nonlinear Systems*. , Engelwood Cliffs, NJ, 2002.

[54] Vincent Denoël. Limit analysis of the statistics of quasi-steady non-linear aerodynamic forces for small turbulence intensities. *Probabilistic Engineering Mechanics*, 24(4):552–564, 2009. doi: DOI: 10.1016/j.probengmech.2009.04.001.